Endogenous p53 expression in human and mouse is not regulated by its 3′UTR

Sibylle Mitschka and Christine Mayr*

Cancer Biology and Genetics Program, Memorial Sloan Kettering Cancer Center, New York, NY 10065, USA

*Correspondence: mayrc@mskcc.org

Christine Mayr
Memorial Sloan Kettering Cancer Center
1275 York Ave, Box 303
New York, NY 10065
Phone: 646-888-3115

Abstract

The *TP53* gene encodes the tumor suppressor p53, which is functionally inactivated in many human cancers. Numerous studies found that overexpression of specific microRNAs or RNA-binding proteins can alter p53 expression through binding to *cis*-regulatory elements in the *TP53* 3′ untranslated region (3′UTR). Although these studies suggested that 3′UTR-mediated p53 expression regulation could play a role in tumorigenesis or could be exploited for therapeutic purposes, they did not investigate post-transcriptional regulation of the native *TP53* gene. We used CRISPR/Cas9 to delete the human and mouse p53 3′UTRs while preserving endogenous mRNA processing. This revealed that the endogenous 3′UTR is not involved in regulating p53 mRNA or protein expression neither in steady state nor after genotoxic stress. As we were able to confirm the previously observed repressive effects of the isolated 3′UTR in reporter assays, our data highlight the importance of genetic models in the validation of post-transcriptional gene regulatory effects.

31 ## Introduction

32 The transcription factor p53 coordinates the cellular stress response. p53 regulates expression
33 of genes involved in cell cycle control, DNA repair, apoptosis, metabolism, and cell
34 differentiation (Kastenhuber and Lowe, 2017). Reduced levels or insufficient p53 activity are
35 major risk factors for the development of cancer and more than half of all human cancers exhibit
36 diminished p53 expression or function (Kastenhuber and Lowe, 2017). In contrast, hyperactive
37 p53 has been linked to impaired wound healing, obesity and accelerated aging (Rufini et al.,
38 2013). These phenomena highlight the importance of p53 protein abundance and activity
39 regulation in human health. p53 protein abundance is primarily controlled by a regulatory
40 feedback loop involving the ubiquitin ligase MDM2. In addition, post-translational modifications
41 of p53 and cofactor recruitment regulate its transcriptional activity (Hafner et al., 2019).

42 The 3′UTR of the *TP53* mRNA is another widely studied element of p53 expression regulation.
43 Apart from facilitating pre-mRNA processing, 3′UTRs can also recruit microRNAs (miRNAs),
44 RNA-binding proteins, and lncRNAs to modulate mRNA stability and protein translation (Tian
45 and Manley, 2017; Mayr, 2019). The human p53 3′UTR contains experimentally characterized
46 binding sites for 23 miRNAs, one lncRNA, and six RNA-binding proteins (Haronikova et al.,
47 2019). A large number of experiments demonstrated the repressive nature of the *TP53* 3′UTR
48 using reporter assays under steady state conditions (Table 1) (Haronikova et al., 2019). In
49 addition, the *TP53* 3′UTR was shown to facilitate an increase in p53 translation after genotoxic
50 stress (Fu and Benchimol, 1997; Mazan-Mamczarz et al., 2003; Chen and Kastan, 2010). This
51 large body of work strongly suggested that miRNAs and RNA-binding proteins prevent p53
52 hyperactivation under normal conditions and induce p53 protein translation after exposure to
53 genotoxic stress (Fu and Benchimol, 1997; Mazan-Mamczarz et al., 2003; Chen and Kastan,
54 2010). However, these claims have not been investigated under native conditions using the
55 endogenous *TP53* mRNA.

56 Here, we generated human cell lines and mice using CRISPR/Cas9 to delete the *TP53* and
57 *Trp53* 3′UTRs at orthologous human and mouse gene loci while keeping mRNA processing
58 intact. In HCT116 cells and in mouse tissues, we did not observe 3′UTR-dependent differences
59 in p53 mRNA or protein levels under normal conditions or after DNA damage. When using the
60 *TP53* 3′UTR in isolation, we confirmed the previously observed repressive effects in reporter
61 assays. However, adding the p53 coding region to the reporters had a substantially stronger
62 repressive effect on expression than the 3′UTR. Moreover, the presence of the p53 coding
63 region prevented repression by the 3′UTR.

64 # Results

65 **Removal of the endogenous 3′UTR does not alter p53 mRNA or protein expression**

66 3′UTRs perform two general functions: They contain regulatory elements that enable mRNA 3′
67 end processing and they harbor elements that allow post-transcriptional gene regulation
68 (Matoulkova et al., 2012). 3′ end processing is essential for the generation of mature mRNAs
69 and is facilitated by the poly(A) signal together with surrounding sequence elements that bind
70 the polyadenylation machinery (Martin et al., 2012). Based on the binding motifs of
71 polyadenylation factors, we consider 100-150 nucleotides upstream of the cleavage site as
72 essential (Martin et al., 2012). Because the human *TP53* 3′UTR has a total length of about
73 1,200 nucleotides, the additional sequence could enable regulatory functions mediated by
74 miRNAs and RNA-binding proteins. Indeed, the vast majority of previously characterized binding
75 sites for miRNAs and RNA-binding proteins are located in the upstream, non-essential part of
76 the *TP53* 3′UTR (Figure 1a, Table 1).

77 To investigate the role of the endogenous human *TP53* 3′UTR in post-transcriptional p53
78 regulation, we used a pair of CRISPR/Cas9 guide RNAs to delete the non-essential part of the
79 3′UTR in HEK293 cells and in the human colon carcinoma cell line HCT116, an established
80 model for investigating p53-dependent functions (Figure 1a, blue and Figure 1-supplement 1a).
81 The homozygous 3′UTR deletion, called ΔUTR (dUTR), removed 1,048 nucleotides,
82 corresponding to 88% of the 3′UTR in wild-type (WT) cells. The deletion affected almost all
83 previously reported binding sites for regulatory miRNAs, lncRNAs, and RNA-binding proteins
84 (Figure 1a, Table 1). We confirmed intact 3′ end processing of the mRNA by northern blot
85 analysis and observed expression of the expected shorter *TP53* mRNA in dUTR cells (Figure
86 1b). We analyzed several HCT116 cell clones carrying a homozygous deletion of the *TP53*
87 3′UTR for p53 mRNA and protein expression and did not observe any differences in steady
88 state cultivation conditions (Figures 1c and 1d). The same was true for HEK293 cells carrying
89 the homozygous dUTR deletion (Figure 1-supplements 1b and 1c).

90

91 **The endogenous 3′UTR is not involved in regulating p53 levels after stress**

92 While p53 mRNA expression does not change upon DNA damage, upregulation of p53 protein
93 expression is achieved through higher translation rates and lower protein turnover (Kumari et
94 al., 2014). Previous studies had suggested a role of the 3′UTR in the upregulation of p53
95 translation after exposure to genotoxic stress (Fu and Benchimol, 1997; Mazan-Mamczarz et

96 al., 2003; Chen and Kastan, 2010). To assess stress-induced p53 expression regulation in
97 dUTR cells, we treated cells with the topoisomerase inhibitor etoposide. We found that
98 concentration-dependent upregulation of p53 protein expression was equal in WT and dUTR
99 cells (Figure 2a). In addition, p53 levels analyzed over two days revealed similar p53 expression
100 kinetics (Figure 2b). Finally, we tested additional stress stimuli including Nutlin-3 (an inhibitor of
101 MDM2), 5-fluorouracil (a thymidylate synthase inhibitor) or UV irradiation. All of these treatments
102 resulted in robust upregulation of p53 protein, but with no detectable differences in p53
103 expression between WT and dUTR cells (Figure 2c). We therefore concluded that the
104 endogenous p53 3′UTR is not required for p53 expression regulation either in steady state or
105 after DNA damage.

106

107 **3′UTR-mediated effects on reporter gene expression are context-dependent**

108 We tried to reconcile our own findings using a genetic model with the existing studies
109 suggesting a repressive function of the 3′UTR. Notably, earlier studies that investigated 3′UTR-
110 dependent p53 regulation used reporter genes as proxy for endogenous p53 regulation (Table
111 1). We therefore cloned the human *TP53* 3′UTR (1,207 nucleotides) or the dUTR fragment (157
112 nucleotides) downstream of GFP and expressed these constructs in p53-/- HCT116 cells
113 (Figure 3a, Figure 3- figure supplement 1a). In the context of the reporter, the *TP53* 3′UTR
114 significantly reduced expression of both GFP mRNA and protein (Figures 3b and 3c). This result
115 was recapitulated when luciferase was used instead of GFP reporters, thus confirming previous
116 findings (Figure 3- figure supplement 1b). We wondered whether the endogenous sequence
117 context could explain these discrepancies and added the p53 coding region (CDS) to our
118 reporter constructs. As expected, we found that the CDS-GFP fusion protein was expressed at
119 much lower levels than GFP alone, which could be due to high p53 turnover caused by MDM2.
120 Surprisingly though, the p53 CDS also drastically suppressed expression of the reporter mRNA
121 indicating a strong contribution of the CDS to p53 mRNA stability regulation (Figure 3c).
122 Importantly, addition of the *TP53* 3′UTR in the context of the CDS did not further repress mRNA
123 or protein expression of the GFP reporter, thus abrogating the difference between the samples
124 containing the dUTR or full-length 3′UTR (Figure 3c). These results reveal that the *TP53* 3′UTR
125 and CDS functionally interact in the regulation of p53 expression and that individual effects
126 cannot be assumed to be additive.

127

128 **A Trp53 dUTR mouse model reveals 3′UTR-independent p53 expression *in vivo***

129 We reasoned that 3′UTR-dependent p53 expression regulation might still play a role in certain
130 developmental stages, tissues or cell types. In order to explore this possibility, we created an
131 analogous mouse model to investigate the role of the p53 3′UTR in an organism. We used
132 zygotic injection of a pair of CRISPR/Cas9 guide RNAs to create mice in which we deleted the
133 non-essential part of the mouse *Trp53* 3′UTR (Figure 4a). After backcrossing, we analyzed
134 *Trp53* dUTR mice harboring a homozygous 3′UTR deletion (Figure 4-supplements 1a-c). These
135 mice were viable, fertile, and did not show any developmental defects (Figure 4-supplements 1d
136 and 1e). We measured *Trp53* mRNA expression in ten different tissues and did not detect
137 significant differences between samples derived from WT and dUTR mice (Figure 4b). To
138 examine the role of the 3′UTR in the regulation of stimulus-dependent p53 expression, we
139 performed total body irradiation of WT and dUTR mice. At four hours post-irradiation, p53
140 protein expression was upregulated to a similar extent in spleen, liver, and colon samples from
141 WT and dUTR mice (Figure 4c). We also analyzed expression of *Cdkn1a,* a highly dosage-
142 sensitive p53 target gene that encodes the cell cycle regulator p21 (Fischer, 2019). Four hours
143 after irradiation, *Cdkn1a* mRNA level were equally induced in WT and dUTR mice, suggesting
144 that p53 target gene activation is 3′UTR-independent in mouse tissues (Figure 4d). These
145 results demonstrate that the non-essential part of the *Trp53* 3′UTR is not required for steady
146 state or stimulus-dependent regulation of p53 mRNA or protein level in mice.

147

148 ## Discussion

149 3′UTRs play important roles in the regulation of mRNA and protein abundance as well as in
150 specifying protein functions (Mayr, 2019). A number of studies have previously proposed that
151 the p53 3′UTR may be required to maintain low expression levels of p53 in non-stressed
152 conditions (Haronikova et al., 2019). Especially miRNAs targeting p53 were previously
153 established as putative gatekeepers to prevent p53 hyperactivation. In addition, some of these
154 miRNAs are also elevated in cancer, e.g. miR-504, miR-30d, and miR-125 (Hu et al., 2010; Li et
155 al., 2012; Banzhaf-Strathmann and Edbauer, 2014). This has sparked an interest in exploiting
156 these mechanisms for therapeutic applications to modulate p53 expression level using novel
157 miRNA-based approaches (Kasinski and Slack, 2011; Hermeking, 2012).

158 The lack of experimental data for 3′UTR-mediated expression regulation in native gene contexts
159 has been a longstanding problem in the field of post-transcriptional gene regulation. Until

160 recently, research on 3′UTR functions has mostly been conducted using overexpression
161 systems and reporter gene assays. In contrast, gene knockouts that disrupt proteins have long
162 been considered the gold standard for analyzing gene functions. The advent of CRISPR/Cas9
163 gene editing tools has made the creation of 3′UTR knockouts using genomic deletion feasible in
164 both cell lines and organisms.

165 Using these tools, we observed that the endogenous p53 3′UTR does not have a significant
166 impact on p53 abundance regulation. While we could reproduce earlier reporter studies with
167 regards to a repressive function of the 3′UTR in isolation, we found that the 3′UTR-mediated
168 repressive effect was abrogated in the context of the p53 coding region. This phenomenon may
169 be explained by differences in RNA folding which could create constraints on motif accessibility.
170 Our results indicate that the different parts of mRNAs do not act autonomously, but are part of a
171 regulatory unit and functionally cooperate with each other (Cottrell et al., 2017; Theil et al.,
172 2019). Notably, a recent study that deleted 3′UTR sequences in several cytokine genes found
173 similar discrepancies between reporter-based assays and gene expression from native contexts
174 (Zhao et al., 2017). Although our data indicate that p53 abundance regulation is 3′UTR-
175 independent, the 3′UTR may still have important functions possibly through control of protein
176 localization or protein activity as has been shown for other proteins (Berkovits and Mayr, 2015;
177 Moretti et al., 2015; Terenzio et al., 2018; Lee and Mayr, 2019; Fernandes and Buchan, 2020;
178 Bae et al., 2020; Kwon, 2020; Mayr, 2019).

179 Our observations further support the recently established role of the coding region as a major
180 regulator of mRNA stability and translation (Mauger et al., 2019; Wu et al., 2019; Narula et al.,
181 2019). Genome-wide comparisons of human coding regions showed that codon optimality and
182 RNA structure in coding regions have the potential to modulate mRNA stability and translation
183 efficiency to a similar extent as 3′UTRs.

184 RNA-binding proteins and miRNAs often target several members of a pathway (Ben-Hamo and
185 Efroni, 2015; Zanzoni et al., 2019). Therefore, the results of overexpression or knockdown
186 experiments of putative 3′UTR regulators may be confounded by other targets that might cause
187 indirect effects. This issue might have contributed to the hypothesis of direct 3′UTR-dependent
188 p53 regulation. For example, the tumor suppressor RBM38 (RNPC1) was proposed to bind to
189 the human *TP53* 3′UTR resulting in lower p53 expression in the presence of RBM38 (Zhang et
190 al., 2011). However, apart from p53, RBM38 targets several other genes in the p53 pathway,
191 including *MDM2*, *PPMID*, and *CDKN1A* (Xu et al., 2013; Zhang et al., 2015; Shu et al., 2006).
192 Expression changes of these genes can indirectly cause p53 expression regulation or result in

193 phenotypes that mimic p53 overexpression. Indeed, while RBM38 knockout mice show
194 phenotypes consistent with p53 hyperactivation (Zhang et al., 2014), Trp53 dUTR mice are
195 apparently normal. This suggests that the repressive effects on p53 that were previously
196 attributed to be mediated by 3′UTR-dependent abundance regulation may be indirect events.

197 Our data imply that in order to develop useful approaches for therapeutic intervention targeting
198 post-transcriptional expression regulation, we need to develop a better understanding of these
199 multi-layered regulatory networks. Our study shows that genetic manipulation of endogenous
200 3′UTRs may be a vital tool to disentangle direct from indirect post-transcriptional effects. It
201 should become an essential step during the testing of miRNA-based therapies that are currently
202 being explored as anti-cancer therapeutics in the context of p53 to avoid mixed or negative
203 results in large clinical trials (Kasinski and Slack, 2011; Hermeking, 2012; Bonneau et al., 2019).

204

205 # Methods

206 **Generation of the *Trp53* dUTR mouse strain using CRISPR/Cas9**

207 Female C57Bl/6 mice between 3-4 weeks of age were superovulated by intraperitoneal injection
208 of Gestyl followed by human chorionic gonadotropin according to standard procedures
209 (Behringer, 2014). After superovulation, the females were setup with male studs for mating.
210 After mating, fertilized eggs were recovered at the one-cell stage from oviducts of superovulated
211 female mice. 1-2 pl of CRISPR/Cas9 RNP complexes were injected into the pronuclei of
212 fertilized eggs (see details below). Surviving eggs were surgically reimplanted into the oviducts
213 of pseudo-pregnant females previously primed for pregnancy by mating with vasectomized
214 males. The resulting pubs were screened using PCR for the deletion amplicon at two weeks of
215 age (primers are listed in Supplementary Table 1). Suitable candidates were further validated by
216 sequencing.

217 <u>Preparation of CRISPR-Cas9 RNP injection mixture.</u> Two target-specific crRNAs and a
218 tracrRNA were purchased from IDT (Supplementary Table 1). In two separate tubes, 2.5 µg of
219 each crRNA was mixed with 5 µg tracrRNA, heated to 95 °C for 5 min and then slowly cooled
220 down to room temperature for annealing. The annealed duplexes were combined and mixed
221 with 1 µg recombinant Cas9 enzyme (PNABIO) and 625 ng *in vitro* transcribed Cas9 mRNA and
222 the total volume was adjusted to 50 µl with sterile water.

223 <u>Screening for homozygous and heterozygous dUTR mice.</u> Two heterozygous founder males

224 with an identical 295 nucleotide deletion (Figure 4-figure supplement 1c) were used to establish
225 a mouse colony. Two or more rounds of backcrossing into wildtype C57Bl/6 mice were
226 performed prior to analysis of *Trp53* dUTR mouse phenotypes. Mouse genotypes from tail
227 biopsies were determined using RT-PCR with specific probes designed for each Trp53 allele
228 (Transnetyx, Cordova, TN).

229 Irradiation of mice. Where indicated, adult mice underwent total body irradiation with 2 or 8 Gy
230 using a Cs-137 source in a Gammacell 40 Exactor (MDS Nordion) at 77 cGy/min. Four hours
231 later irradiated mice were euthanized to collect samples. All procedures were approved by the
232 Institutional Animal Care and Use Committee at MSKCC under protocol 18-07-010.

233 **Extraction of total RNA from mouse tissues and human cells for RT-qPCR analysis**

234 For RNA extraction from mouse tissue, freshly collected tissue samples were flash-frozen and
235 transferred to RNAlater-ICE Frozen Tissue Transition Solution (Invitrogen). After soaking
236 overnight at -20 °C, the tissue samples were homogenized in vials containing 1.4 mm ceramic
237 beads (Fisherbrand) and 400 µl RLT buffer (Qiagen) using a bead mill (Bead Ruptor 24,
238 Biotage). 200 µl of the tissue homogenate was mixed with 1 ml of TRI Reagent (Invitrogen). For
239 extraction of RNA from cultured cells, the cell pellet was directly resuspended in TRI Reagent.
240 Total RNA extraction was performed according to the manufacturer's protocol. The resulting
241 RNA was treated with 2U DNaseI enzyme (NEB) for 30 min at 37 °C, followed by acidic phenol
242 extraction and isopropanol precipitation. To generate cDNA, about 200 ng of RNA was used in a
243 reverse transcription reaction with SuperScript IV VILO Master Mix (Invitrogen). To measure the
244 relative expression levels of mRNAs by RT-qPCR, FastStart Universal SYBR Green Master
245 (ROX) from Roche was used together with gene-specific primers listed in Supplementary Table
246 1. GAPDH/Gapdh was used as reference gene.

247 **Generation of the *TP53* 3′UTR deletion in HCT116 and HEK293 cells**

248 To generate CRISPR/Cas9 constructs, we annealed target-specific gRNA sequences and
249 inserted them into a BbsI-digested pX330-U6-Chimeric_BB-CBh-hSpCAs9 vector (Addgene
250 plasmid #42230) (Cong et al., 2013; Ran et al., 2013). 1 µg of each pX330-gRNA plasmid plus
251 0.1 µg of pmaxGFP plasmid (Lonza) were transiently transfected into exponentially growing
252 cells using Lipofectamine 2000 (Invitrogen). Three days after transfection, single GFP-positive
253 cells were sorted into 96-well plates and cultured until colonies formed. The genomic DNA from
254 individual cell clones was extracted using QuickExtract DNA Extraction Solution (Lucigen) and
255 screened by PCR for the deletion amplicon using the DNA primers listed in Supplementary

256 Table 1. In the case of HCT116 cells, we repeated the above-described process using two
257 different heterozygous clones with a new downstream gRNA to obtain homozygous *TP53* dUTR
258 cells. Finally, to validate positive cell clones, all *TP53* alleles of candidate clones were
259 sequenced (Figure 1-supplement 1a).

260 **Generation of p53 KO HCT116 and HEK293 cells**

261 We generated our own p53-deficient HEK293 and HCT116 cell lines by targeting exon 6 of the
262 p53 coding region with a gRNA causing frame shift mutations. Specifically, pX330 plasmid
263 harboring a p53-specific gRNA (Supplementary Table 1) was transfected into HEK293 and
264 HCT116 cells using Lipofectamine 2000 (Invitrogen). Two days later, the cells were split and
265 seeded sparsely on a 10 cm dish in the presence of 10 μM Nutlin-3 (Seleckchem) which was
266 used to select against growth of p53-competent cells. After ten days, single colonies were
267 picked, and individual clones were validated by WB for loss of p53 expression.

268 **Western blot analysis**

269 RIPA buffer (10 mM Tris-HCL pH 7.5, 150 mM NaCl, 0.5 mM EDTA, 0.1% SDS, 1% Triton X-
270 100, 1% deoxycholate, Halt Protease Inhibitor Cocktail (Thermo Scientific)) was used to extract
271 total protein from cultured cells or mouse tissues. Cell pellets were washed with PBS and
272 directly resuspended in lysis buffer and incubated on ice for 30 min. Mouse tissue samples were
273 homogenized in RIPA buffer using a bead mill in vials filled with 1.4 mm ceramic beads. Tissue
274 lysates were sonicated to shear genomic DNA prior to removing insoluble components by
275 centrifugation (10 min, 15,000 g). The proteins in the supernatant were precipitated by adding
276 0.11 volumes of ice-cold 100 % Trichloroacetic acid (TCA) and incubated at -20 °C for one hour.
277 The samples were centrifuged (10 min, 15,000 g) and the pellet was washed twice in ice-cold
278 acetone before resuspending in reducing 2x Laemmli buffer (Alfa Aesar). Proteins were
279 separated by size on a 4-12% Bis-Tris SDS-PAGE gels (Invitrogen) and blotted on a 0.2 μm
280 nitrocellulose membrane (BIO-RAD). The membrane was then incubated with primary antibody
281 in Odyssey Blocking buffer (LI-COR) overnight at 4 °C. The following primary antibodies were
282 used in this study: anti-human p53 (Santa Cruz, sc-47698, mouse, 1:250), anti-mouse p53 (Cell
283 Signaling, #2524, mouse, 1:500), anti-Actin (Sigma, A2008, rabbit, 1:1000), anti-Tubulin (Sigma,
284 T9026, mouse 1:1000) and anti-GAPDH (Sigma, G8705, mouse, 1:1000). After washing, the
285 membrane was incubated with fluorescently-labeled secondary antibodies (IRDye 800CW Goat
286 anti-Mouse, 926-32210; IRDye 680 Goat anti-Rabbit, 926-68071 LI-COR) and signals were
287 recorded using the Odyssey Infrared Imaging system (LI-COR).

288 **Northern Blot**

289 Total RNA from cells was extracted as described above. Afterwards, polyA+ mRNA was
290 enriched from total RNA using the Oligotex suspension (Qiagen) according to the
291 manufacturer's instructions. 1.2 µg of polyA+ mRNA was glyoxylated and run on an agarose gel
292 as described previously (Mayr and Bartel, 2009). The RNA was transferred overnight using the
293 Nytran SuPerCharge TurboBlotter system (Whatman) and UV-crosslinked.

294 DNA probes complementary to the *TP53* coding region or the 3′UTR were labeled with dCTP [α-
295 ^{32}P] using the Amersham Megaprime DNA labeling system (GE Healthcare). Primers used for
296 probe synthesis from human cDNA are listed in Supplementary Table 1. Labeled probes were
297 denatured by heat for 5 min at 90 °C and then incubated with the blot in ULTRAhyp
298 Ultrasensitive Hybridization Buffer (Invitrogen) overnight at 42 °C. The blot was washed three
299 times and exposed on a phosphorimaging screen. The radioactive signal was acquired using
300 the Fujifilm FLA700 phosphorimager.

301 **Human cell culture and drug treatment**

302 Human cell cultures were maintained in a 5% CO_2/ 37 °C humidified environment. HEK293 cells
303 were cultured in DMEM (high glucose) and HCT116 cells were cultured in McCoy's 5A medium
304 which were supplemented with 10% FBS and 1% Penicillin/Streptomycin. Where indicated,
305 HCT116 cells were treated with etoposide (0.125-32 µM, Sigma), 5-fluorouracil (40 µM, Sigma),
306 Nutlin-3 (20 µM, Seleckchem), or UV (50 J/m^2) prior to downstream analysis.

307 **Reporter assays**

308 We PCR-amplified the *TP53* 3′UTR sequence (nucleotides 1,380 to 2,586 of the reference
309 mRNA NM_000546, May 2018) from WT HCT116 cDNA. This sequence was cloned
310 downstream of the stop codon in pcDNA3.1-puro-eGFP using EcoRI/NotI restriction enzymes.
311 For the dUTR construct, cDNA from TP53 dUTR HCT116 cells was used to amplify the
312 remaining 3′UTR sequence after CRISPR-mediated deletion, representing a fusion of the first
313 12 and the last 157 nucleotides of the *TP53* 3′UTR. The p53 coding region, encoding the α
314 protein isoform (1,182 nucleotides), was cloned upstream and in frame of the GFP-cassette
315 using HindIII/BamHI restriction sites. For luciferase reporter studies, the full length 3′UTR and
316 dUTR sequences described above were cloned into a SmaI-digested psiCHECK2 (Promega)
317 vector via blunt-end cloning.

318 <u>GFP reporter.</u> GFP protein levels of cells transfected with equimolar amounts of GFP-containing
319 reporter constructs was analyzed by flow cytometry after 24 hours. A BD LSRFortessa Flow

320 Cytometer was used to record the mean fluorescence intensity (MFI) of 20,000 life cells. Raw
321 data were analyzed using the FlowJo software package and values were normalized to GFP-
322 only constructs. mRNA abundance of the GFP reporter was measured using RT-qPCR using
323 the primers listed in Supplementary Table 1. The GFP reporter mRNA was normalized to
324 *GAPDH* mRNA.

325 Luciferase reporter assay. Luciferase activity was measured 24 hours after transfection of
326 equimolar amounts of psiCHECK2 plasmids (Promega) containing either the *TP53* 3′UTR or
327 dUTR sequence downstream of the Renilla luciferase translational stop codon. Cells were lysed
328 in passive lysis buffer and Renilla and firefly luciferase activity was measured in duplicates
329 using the Dual-Glo Luciferase Assay System (Promega) according to the manufacturer's
330 instructions in a GloMax 96 Microplate Luminometer (Promega). Relative light units of Renilla
331 luciferase were normalized to firefly luciferase activity.

332 **Statistics and reproducibility**

333 Statistical analysis of the mRNA and protein expression data was performed using a Student's t-
334 test or ANOVA followed by a Tukey's multiple comparison test. We use ns ($p > 0.05$), *
335 $0.01 < p < 0.05$, ** $0.001 < p < 0.01$, and *** $p < 0.001$ to indicate the levels of p-values in figures.
336 No data were excluded. The results for immunoblotting are representative of at least three
337 biologically independent experiments. All statistical analyses and visualizations were performed
338 by using GraphPad (Prism 8).

339

340 **Acknowledgements**

341 We thank all members of the Mayr lab for helpful discussions and critical reading of the
342 manuscript. We thank the Mouse Genetics Core Facility at MSKCC for assistance in the
343 generation of Trp53 dUTR mice. This work was funded by a postdoctoral fellowship from the
344 DFG to S.M. and by the NIH Director′s Pioneer Award (DP1-GM123454), the Pershing Square
345 Sohn Cancer Research Alliance to C.M., and the NCI Cancer Center Support Grant (P30
346 CA008748). The funders had no role in study design, data collection and interpretation, or the
347 decision to submit the work for publication.

348 **Author contributions**

349 S.M. performed all experiments and analyses. S.M. and C.M. conceived the project, designed
350 the experiments, and wrote the manuscript.

351 **Declaration of Interests**

352 The authors declare no competing interests.

353 **Additional files**

354 Supplementary Table 1. Primer sequences

355 Transparent Reporting Form

356 **Data availability**

357 All data generated and analyzed are included in the manuscript and supporting files.

358

359 **References**

360 Bae, B., Gruner, H.N., Lynch, M., Feng, T., So, K., Oliver, D., Mastick, G.S., Yan, W., Pieraut,
361 S., and Miura, P. (2020). Elimination of Calm1 long 3'-UTR mRNA isoform by CRISPR-
362 Cas9 gene editing impairs dorsal root ganglion development and hippocampal neuron
363 activation in mice. RNA *26*, 1414-1430.
364 Banzhaf-Strathmann, J., and Edbauer, D. (2014). Good guy or bad guy: the opposing roles of
365 microRNA 125b in cancer. Cell communication and signaling : CCS *12*, 30.
366 Behringer, R., Gertsenstein, M., Nagy, K., Nagy, A. (2014). Manipulating the Mouse Embryo: A
367 Laboratory Manual, Fourth Edition (CSH press).
368 Ben-Hamo, R., and Efroni, S. (2015). MicroRNA regulation of molecular pathways as a generic
369 mechanism and as a core disease phenotype. Oncotarget *6*, 1594-1604.
370 Berkovits, B.D., and Mayr, C. (2015). Alternative 3' UTRs act as scaffolds to regulate membrane
371 protein localization. Nature *522*, 363-367.
372 Bonneau, E., Neveu, B., Kostantin, E., Tsongalis, G.J., and De Guire, V. (2019). How close are
373 miRNAs from clinical practice? A perspective on the diagnostic and therapeutic market.
374 Ejifcc *30*, 114-127.
375 Chen, J., and Kastan, M.B. (2010). 5'-3'-UTR interactions regulate p53 mRNA translation and
376 provide a target for modulating p53 induction after DNA damage. Genes Dev *24*, 2146-
377 2156.
378 Cong, L., Ran, F.A., Cox, D., Lin, S., Barretto, R., Habib, N., Hsu, P.D., Wu, X., Jiang, W.,
379 Marraffini, L.A.*, et al.* (2013). Multiplex genome engineering using CRISPR/Cas
380 systems. Science *339*, 819-823.
381 Cottrell, K.A., Szczesny, P., and Djuranovic, S. (2017). Translation efficiency is a determinant of
382 the magnitude of miRNA-mediated repression. Sci Rep *7*, 14884.
383 Fernandes, N., and Buchan, J.R. (2020). RPS28B mRNA acts as a scaffold promoting cis-
384 translational interaction of proteins driving P-body assembly. Nucleic Acids Res *48*,
385 6265-6279.
386 Fischer, M. (2019). Conservation and divergence of the p53 gene regulatory network between
387 mice and humans. Oncogene *38*, 4095-4109.
388 Fu, L., and Benchimol, S. (1997). Participation of the human p53 3'UTR in translational
389 repression and activation following gamma-irradiation. EMBO J *16*, 4117-4125.
390 Hafner, A., Bulyk, M.L., Jambhekar, A., and Lahav, G. (2019). The multiple mechanisms that
391 regulate p53 activity and cell fate. Nature reviews Molecular cell biology *20*, 199-210.

392 Haronikova, L., Olivares-Illana, V., Wang, L., Karakostis, K., Chen, S., and Fahraeus, R. (2019).
393 The p53 mRNA: an integral part of the cellular stress response. Nucleic Acids Res *47*,
394 3257-3271.
395 Hermeking, H. (2012). MicroRNAs in the p53 network: micromanagement of tumour
396 suppression. Nat Rev Cancer *12*, 613-626.
397 Hu, W., Chan, C.S., Wu, R., Zhang, C., Sun, Y., Song, J.S., Tang, L.H., Levine, A.J., and Feng,
398 Z. (2010). Negative regulation of tumor suppressor p53 by microRNA miR-504. Mol Cell
399 *38*, 689-699.
400 Kasinski, A.L., and Slack, F.J. (2011). Epigenetics and genetics. MicroRNAs en route to the
401 clinic: progress in validating and targeting microRNAs for cancer therapy. Nat Rev
402 Cancer *11*, 849-864.
403 Kastenhuber, E.R., and Lowe, S.W. (2017). Putting p53 in Context. Cell *170*, 1062-1078.
404 Kumari, R., Kohli, S., and Das, S. (2014). p53 regulation upon genotoxic stress: intricacies and
405 complexities. Molecular & cellular oncology *1*, e969653.
406 Kwon, B., Patel, N.D., Lee, S.H., Lee, J., Ma, W., Mayr, C. (2020). Enhancers regulate
407 polyadenylation site cleavage and control 3′UTR isoform expression. bioRxiv, doi:
408 https://doi.org/10.1101/2020.1108.1117.254193.
409 Lee, S.H., and Mayr, C. (2019). Gain of Additional BIRC3 Protein Functions through 3'-UTR-
410 Mediated Protein Complex Formation. Mol Cell *74*, 701-712 e709.
411 Li, N., Kaur, S., Greshock, J., Lassus, H., Zhong, X., Wang, Y., Leminen, A., Shao, Z., Hu, X.,
412 Liang, S.*, et al.* (2012). A combined array-based comparative genomic hybridization and
413 functional library screening approach identifies mir-30d as an oncomir in cancer. Cancer
414 Res *72*, 154-164.
415 Martin, G., Gruber, A.R., Keller, W., and Zavolan, M. (2012). Genome-wide analysis of pre-
416 mRNA 3' end processing reveals a decisive role of human cleavage factor I in the
417 regulation of 3' UTR length. Cell reports *1*, 753-763.
418 Matoulkova, E., Michalova, E., Vojtesek, B., and Hrstka, R. (2012). The role of the 3'
419 untranslated region in post-transcriptional regulation of protein expression in mammalian
420 cells. RNA biology *9*, 563-576.
421 Mauger, D.M., Cabral, B.J., Presnyak, V., Su, S.V., Reid, D.W., Goodman, B., Link, K.,
422 Khatwani, N., Reynders, J., Moore, M.J.*, et al.* (2019). mRNA structure regulates protein
423 expression through changes in functional half-life. Proc Natl Acad Sci U S A *116*, 24075-
424 24083.
425 Mayr, C. (2019). What Are 3' UTRs Doing? Cold Spring Harb Perspect Biol *11*.
426 Mayr, C., and Bartel, D.P. (2009). Widespread shortening of 3'UTRs by alternative cleavage and
427 polyadenylation activates oncogenes in cancer cells. Cell *138*, 673-684.
428 Mazan-Mamczarz, K., Galban, S., Lopez de Silanes, I., Martindale, J.L., Atasoy, U., Keene,
429 J.D., and Gorospe, M. (2003). RNA-binding protein HuR enhances p53 translation in
430 response to ultraviolet light irradiation. Proc Natl Acad Sci U S A *100*, 8354-8359.
431 Moretti, F., Rolando, C., Winker, M., Ivanek, R., Rodriguez, J., Von Kriegsheim, A., Taylor, V.,
432 Bustin, M., and Pertz, O. (2015). Growth Cone Localization of the mRNA Encoding the
433 Chromatin Regulator HMGN5 Modulates Neurite Outgrowth. Mol Cell Biol *35*, 2035-
434 2050.
435 Narula, A., Ellis, J., Taliaferro, J.M., and Rissland, O.S. (2019). Coding regions affect mRNA
436 stability in human cells. RNA *25*, 1751-1764.
437 Ran, F.A., Hsu, P.D., Wright, J., Agarwala, V., Scott, D.A., and Zhang, F. (2013). Genome
438 engineering using the CRISPR-Cas9 system. Nature protocols *8*, 2281-2308.
439 Rufini, A., Tucci, P., Celardo, I., and Melino, G. (2013). Senescence and aging: the critical roles
440 of p53. Oncogene *32*, 5129-5143.

441 Shu, L., Yan, W., and Chen, X. (2006). RNPC1, an RNA-binding protein and a target of the p53
442 family, is required for maintaining the stability of the basal and stress-induced p21
443 transcript. Genes Dev *20*, 2961-2972.
444 Terenzio, M., Koley, S., Samra, N., Rishal, I., Zhao, Q., Sahoo, P.K., Urisman, A., Marvaldi, L.,
445 Oses-Prieto, J.A., Forester, C.*, et al.* (2018). Locally translated mTOR controls axonal
446 local translation in nerve injury. Science *359*, 1416-1421.
447 Theil, K., Imami, K., and Rajewsky, N. (2019). Identification of proteins and miRNAs that
448 specifically bind an mRNA in vivo. Nature communications *10*, 4205.
449 Tian, B., and Manley, J.L. (2017). Alternative polyadenylation of mRNA precursors. Nature
450 reviews Molecular cell biology *18*, 18-30.
451 Wu, Q., Medina, S.G., Kushawah, G., DeVore, M.L., Castellano, L.A., Hand, J.M., Wright, M.,
452 and Bazzini, A.A. (2019). Translation affects mRNA stability in a codon-dependent
453 manner in human cells. eLife *8*.
454 Xu, E., Zhang, J., and Chen, X. (2013). MDM2 expression is repressed by the RNA-binding
455 protein RNPC1 via mRNA stability. Oncogene *32*, 2169-2178.
456 Zanzoni, A., Spinelli, L., Ribeiro, D.M., Tartaglia, G.G., and Brun, C. (2019). Post-transcriptional
457 regulatory patterns revealed by protein-RNA interactions. Sci Rep *9*, 4302.
458 Zhang, J., Cho, S.J., Shu, L., Yan, W., Guerrero, T., Kent, M., Skorupski, K., Chen, H., and
459 Chen, X. (2011). Translational repression of p53 by RNPC1, a p53 target overexpressed
460 in lymphomas. Genes Dev *25*, 1528-1543.
461 Zhang, J., Xu, E., Ren, C., Yan, W., Zhang, M., Chen, M., Cardiff, R.D., Imai, D.M., Wisner, E.,
462 and Chen, X. (2014). Mice deficient in Rbm38, a target of the p53 family, are susceptible
463 to accelerated aging and spontaneous tumors. Proc Natl Acad Sci U S A *111*, 18637-
464 18642.
465 Zhang, M., Xu, E., Zhang, J., and Chen, X. (2015). PPM1D phosphatase, a target of p53 and
466 RBM38 RNA-binding protein, inhibits p53 mRNA translation via dephosphorylation of
467 RBM38. Oncogene *34*, 5900-5911.
468 Zhao, W., Siegel, D., Biton, A., Tonqueze, O.L., Zaitlen, N., Ahituv, N., and Erle, D.J. (2017).
469 CRISPR-Cas9-mediated functional dissection of 3'-UTRs. Nucleic Acids Res *45*, 10800-
470 10810.
471

Table 1. Previously reported evidence of miRNAs, lncRNAs, and RNA-binding proteins that target the p53 3′UTR.

Interactors of the human *TP53* mRNA mapping to the last exon					
Name	**Type**	**Binding region (NM_000546.6)**	**Affected in dUTR allele?**	**Experiments**	**References (PMID)**
miR-1228-3p	miRNA	1422-1428	yes	LRA, RT-qPCR, IHC, WB	25422913
miR-125a-5p	miRNA	2044-2063	yes	LRA, NB, RT-qPCR, WB	19818772
miR-125b-5p	miRNA	2043-2064	yes	LRA, ISH, RT-qPCR, WB	19293287, 21935352, 27592685
miR-1285-3p	miRNA	2113-2134	yes	LRA, RT-qPCR, WB	20417621
miR-150-5p	miRNA	1568-1580	yes	LRA, WB	23747308
miR-151a-5p	miRNA	2304-2325	yes	LRA, ChIP-seq, RT-qPCR, WB	27191259
miR-200a-3p	miRNA	2269-2291	yes	LRA, WB	23144891
miR-24-3p	miRNA	2352-2374	yes	LRA, IHC, RT-qPCR, WB	27780140
miR-25-3p	miRNA	1401-1423	yes	LRA, RT-qPCR, WB	20935678
miR-30d-5p	miRNA	1596-1618	yes	LRA, RT-qPCR, WB	20935678
miR-375	miRNA	1462-1483	yes	LRA, Flow, RT-qPCR, WB, IF	23835407
miR-663a	miRNA	1260-1281	no (in CDS)	LRA	27105517
miR-504	miRNA	2059-2066, 2387-2395	yes, no	LRA, RT-qPCR, WB	20542001
miR-92	miRNA	1417-1422	yes	LRA, WB	21112562
miR-141	miRNA	2285-2290	yes	LRA, WB	21112562
miR-638	miRNA	1381-1404	yes	LRA, WB, IP	25088422
miR-3151	miRNA	1337-1354	yes	LRA, WB, RT-qPCR	24736457
miR-33	miRNA	1957-1980	yes	LRA, WB	20703086
miR-380-5p	miRNA	1909-1936, 1943-1974	yes, yes	LRA, WB	20871609
miR-19b	miRNA	1712-1734	yes	LRA, WB	24742936
miR-15a	miRNA	2394-2414	no	LRA, WB	21205967
miR-16	miRNA	2394-2415	no	LRA, WB	21205967
miR-584	miRNA	1263-1284	no (in CDS)	LRA, WB, IP	25088422
WIG1	RBP	2064-2106	yes	LRA, IP, RT-qPCR	19805223
PARN	RBP	2071-2102	yes	LRA, EMSA, IP, RT-qPCR	23401530
CPEB1	RBP	2458-2500	no	IP, RT-PCR	19141477
RBM38 (RNPC1)	RBP	2064-2106	yes	EMSA, IP, RT-PCR, Polysome gradient	21764855, 24142875, 25823026
RBM24	RBP	2064-2106	yes	LRA, EMSA, IP, RT-qPCR,	29358667
HUR	RBP	2064-2106, 2393-2412, 2458-2505	yes, yes, no	LRA, EMSA, WB, RT-qPCR	12821781, 14517280, 16690610, 18680106
7SL	lncRNA	2107-2149, 2194-2240, 2269-2301, 2307-2362	yes, yes, yes, yes	LRA, IP, WB	25123665

Interactors of the murine *Trp53* mRNA mapping to the last exon					
Name	**Type**	**Binding region (NM_011640.3)**	**Affected in dUTR allele?**	**Experiments**	**References (PMID)**
miR-92a-3p	miRNA	1646-1666	yes	LRA, WB	22451425
Tia1	RBP	1426-1442, 1702-1731	yes, no	LRA, iCLIP	28904350
Hzf	RBP	1345-1395, 1529-1574	yes, yes	LRA, EMSA, WB, IP, RT-qPCR, Polysome gradient	21402775

Abbreviations: LRA: luciferase reporter assay; WB: western blot; IP: co-immunoprecipitation assay; RT-qPCR: quantitative reverse transcription PCR; NB: northern blot; IHC: immunohistochemistry; ISH: In situ hybridization; EMSA: electromobility shift assay.

Mitschka, Figure 1

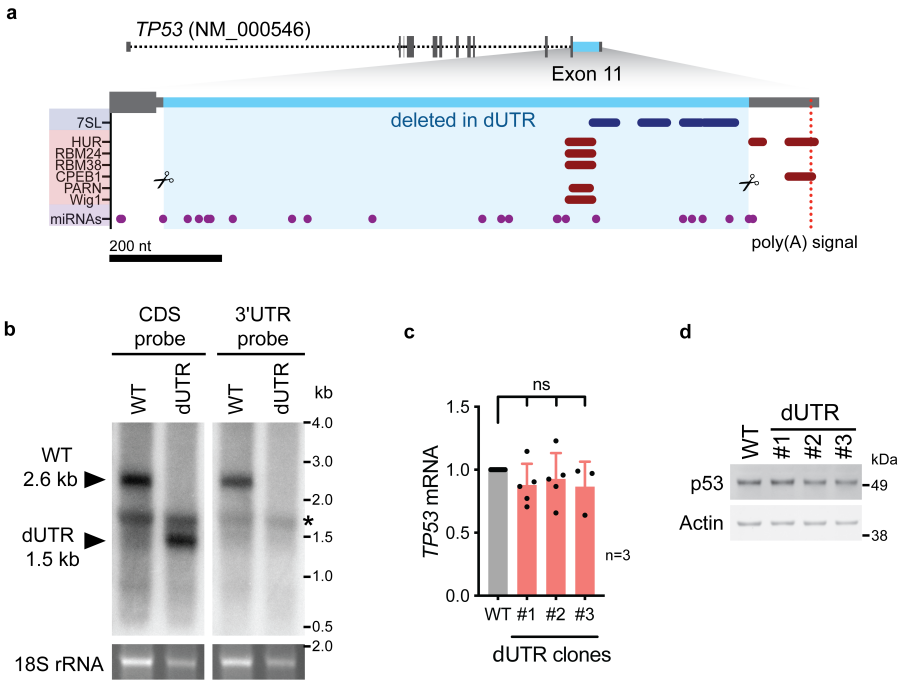

Figure 1. 3′UTR-independent p53 expression regulation in steady state in human cells.
a, Schematic of the human *TP53* gene. The sequence deleted in dUTR cells is shown in blue. Tracks of binding sites for miRNAs, RBPs and lncRNA are depicted below (see also Table 1).
b, Northern blot analysis of *TP53* mRNA from WT and dUTR HEK293 cells. A probe that hybridizes to the *TP53* coding region (CDS) reveals expression of a shortened *TP53* mRNA in dUTR cells. The size difference is consistent with the length of the CRISPR/Cas9-induced deletion. A probe designed to bind the *TP53* 3′UTR does not produce a signal in the mRNA of dUTR cells, confirming removal of this sequence element. The band of 18S rRNA is used as a loading control. * indicates an unspecific band from ribosomal rRNA.
c, *TP53* mRNA expression levels in WT HCT116 cells and three different dUTR cell clones are shown from n=3 independent experiments (mean + s.d.) after normalization to *GAPDH*.
d, As in c, but shown is p53 protein expression. Actin serves as loading control.
See also figure supplement 1 for sequnce alignments and data generated with *TP53* dUTR HEK293 cells.

Mitschka, Figure 1-figure supplement 1

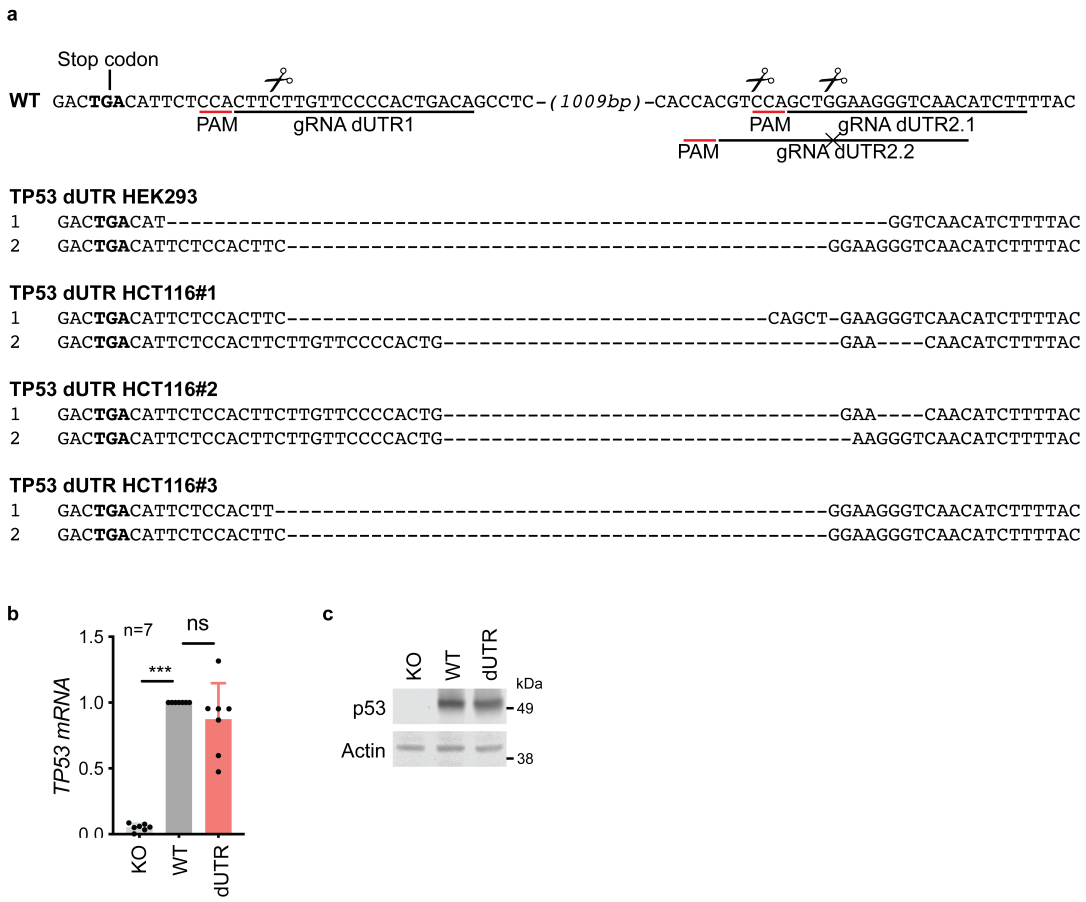

Figure 1-figure supplement 1. Generation and characterization of *TP53* dUTR human cell lines.

a, Sequence alignment of TP53 alleles spanning the deletion sites in WT and dUTR HEK293 and HCT116 cell clones analyzed in this study. Binding sites of gRNAs used to generate the deletion are underlined in the WT reference sequence and predicted cutting sites are marked by a scissor symbol. gRNA dUTR2.2 harboring a specifc point mutation relative to the WT allele was used to create homozygous dUTR HCT116 cell lines during a second round of transfection.
b, Analysis *TP53* mRNA levels in WT, protein KO, and dUTR HEK293 cells was measured by RT-qPCR and normalized with *GAPDH* mRNA levels. Shown are mean + s.d. of n=7 independent experiments.
c, Immunoblot showing p53 protein level in HEK293 cells, grown under steady state conditions.

Mitschka, Figure 2

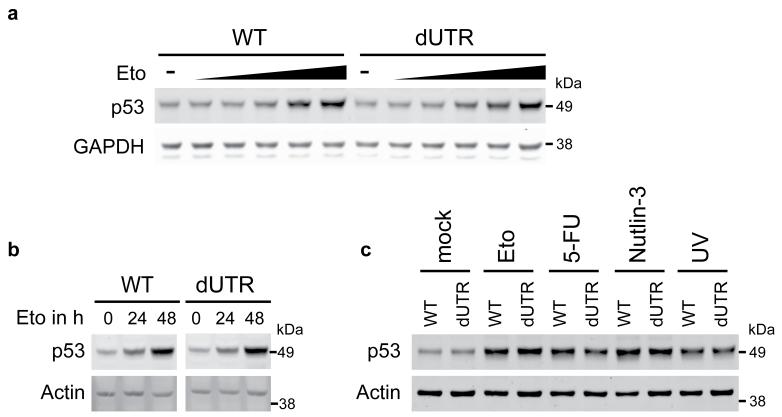

Figure 2. The 3′UTR is not required to induce upregulation of p53 protein after genotoxic stress.

a, Immunoblot showing p53 protein levels after four hours of Etoposide (Eto) treatment (0-32 μM) in WT and dUTR HCT116 cells. GAPDH serves as loading control.

b, WT and dUTR HCT116 ells were treated with 0.5 μM Etoposide for 0, 24 and 48 hours. Actin serves as loading control.

c, As in b, but cells were treated with 20 μM Etoposide, 40 μM 5-Fluorouridine (5-FU), 20 μM Nutlin-3 or 50 J/m^2 UV. Actin serves as loading control.

Mitschka, Figure 3

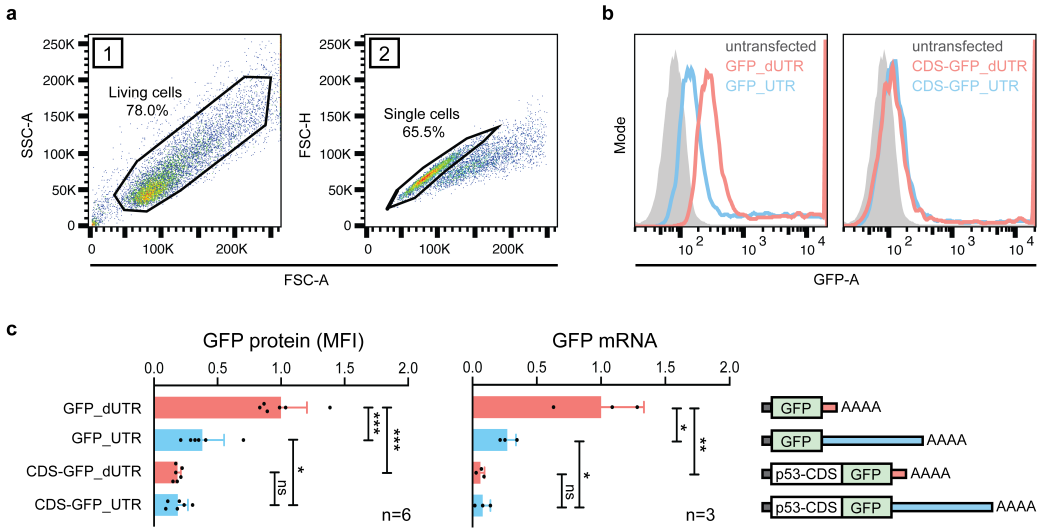

Figure 3. 3′UTR and coding region of p53 have non-additive effects on the expression of a reporter gene.

a, Gating strategy in FACS experiment for measurement of GFP protein expression in p53 -/- HCT116 cells.

b, Histogram plots from one representative FACS experiment. The grey area represents the untransfected, GFP-negative control population.

c, GFP protein levels were quantified by FACS and *GFP* mRNA levels were measured by RT-qPCR using *GAPDH* as housekeeping gene in p53 -/- HCT116 cells. Shown is mean + s.d. of n=3 independent experiments. CDS, coding sequence. Statistical analysis using unpaired Student's t-test with * $p<0.05$, ** $p<0.01$, *** $p<0.0001$; ns not significant.

See also figure supplement 1 for additional information.

Mitschka, Figure 3-figure supplement 1

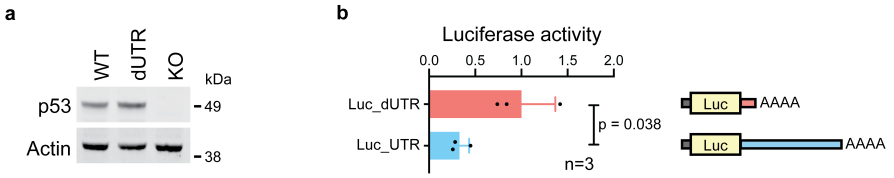

Figure 3-figure supplement 1. Validation of repressive effect of *TP53* 3′UTR in luciferase reporter assay.
a, Immunoblot showing p53 protein level in WT, dUTR and p53-/- HCT116 cells, grown under steady-state conditions.
b, Renilla luciferase activity of constructs containing either the human dUTR or the human full-length *TP53* 3′UTR was performed in p53 -/- HCT116 cells. Shown is mean + s.d. of n=3 independent experiments after normalization to firefly luciferase. Statistical analysis using t-test for independent samples.

Mitschka, Figure 4

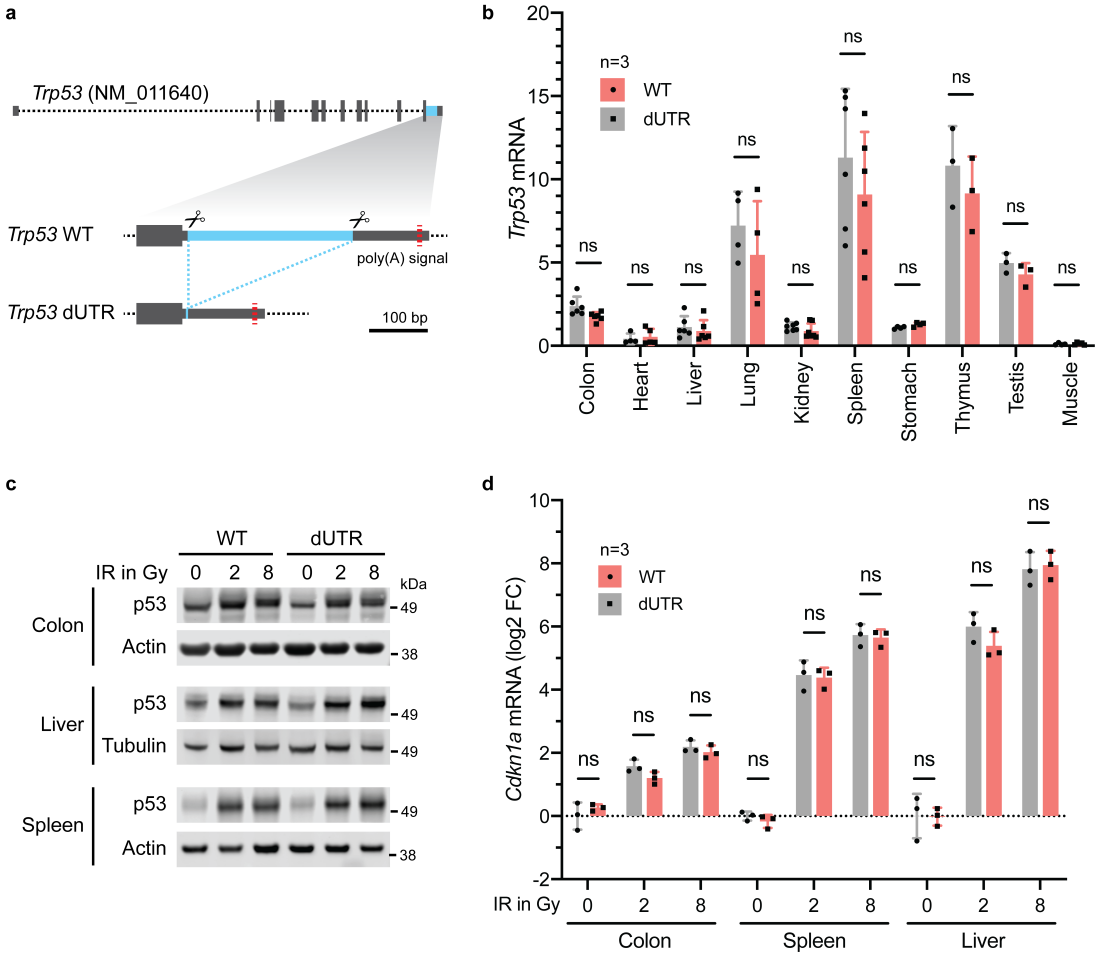

Figure 4. Knockout of the *Trp53* 3′UTR does not lead to aberrant p53 expression in a mouse model.

a, Schematic of the mouse *Trp53* gene. The sequence deleted in dUTR cells is shown in blue.
b, *Trp53* mRNA in tissues from WT and dUTR mice was normalized to *Gapdh*. Shown is mean + s.d. from n=3 independent experiments. See also figure supplement 1 for more information.
c, Representative immunoblots of p53 protein from tissues obtained four hours after total body irradiation. Gy, Gray.
d, *Cdkn1a* mRNA expression of samples from (c) was normalized to *Gapdh*. Shown is mean + s.d. from three mice.

Mitschka, Figure 4-figure supplement 1

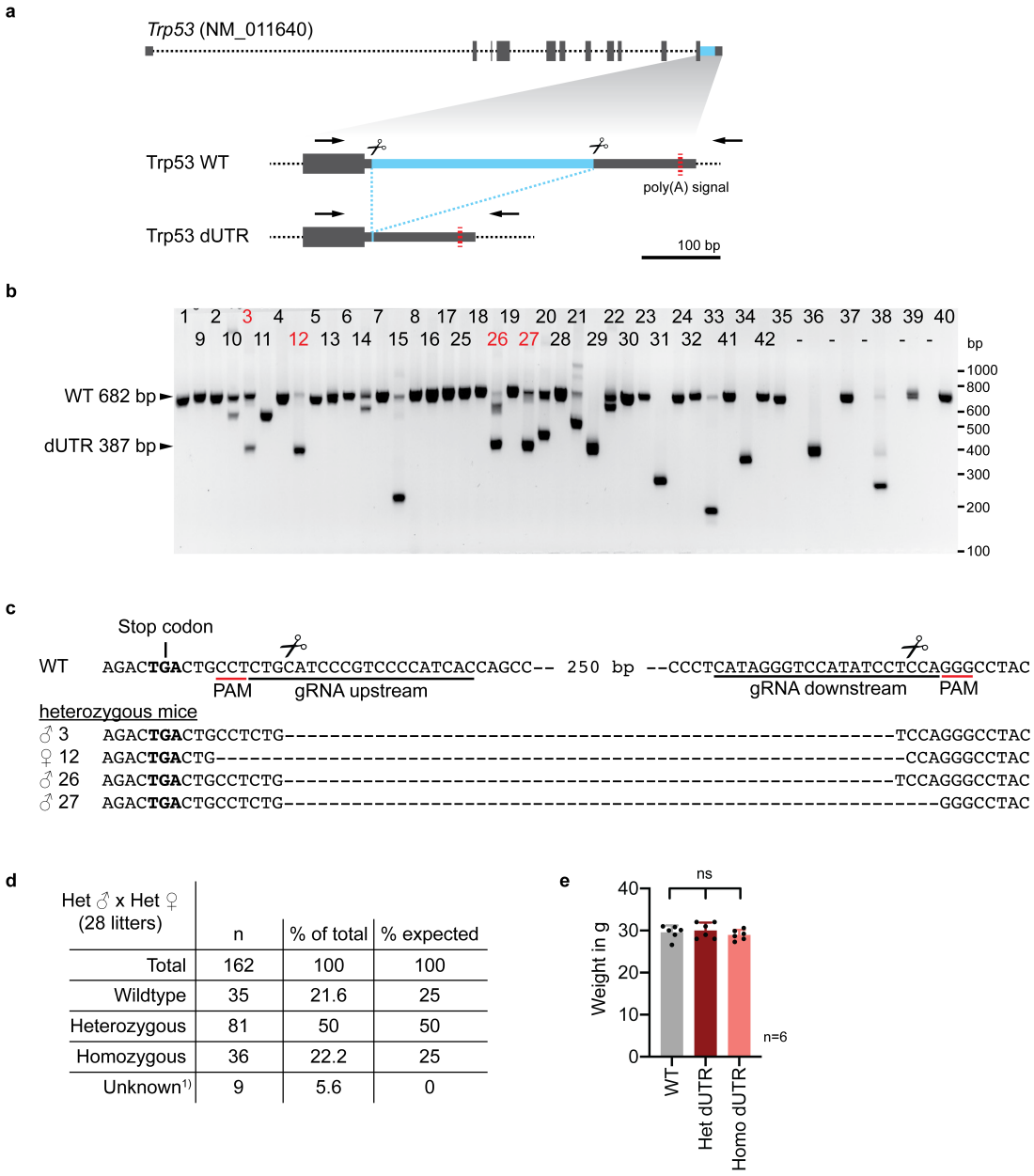

Het ♂ x Het ♀ (28 litters)	n	% of total	% expected
Total	162	100	100
Wildtype	35	21.6	25
Heterozygous	81	50	50
Homozygous	36	22.2	25
Unknown[1)]	9	5.6	0

Figure 4-figure supplement 1. Generation and characterization of *Trp53* dUTR mice.
a, Schematic of the mouse *Trp53* gene. The sequence deleted in dUTR cells is shown in blue and binding sites of primers used for PCR screening are marked with arrows.
b, Screening PCR of mice that were born after zygotic injection of CRISPR/Cas9 RNPs targeting the *Trp53* 3′UTR. The predicted lengths of the PCR products from WT and dUTR alleles are indicated. Mice that were selected for validation by sequencing are labeled in red.
c, Sequence alignments of *Trp53* dUTR alleles of select founder mice shown in b. Male mice #3 and #26 harboring identical DNA deletions were used to establish a mouse colony. Primer sequences used for screening can be found in Supplementary Table 1.
d, Genotypes of pups from 28 *Trp53* dUTR heterozygous intercrosses. Unknown refers to mice that died before weening.
e, Weights of mice at 10-11 weeks of age are shown for WT, *Trp53* dUTR heterozygous and homozygous males. Data are shown as mean + s.d. with n=6 in each group.